separations

MDPI

Article

Green Ultrasonic-Assisted Extraction of Bioactive Phenolic Constituents from *Gastrodia elata*: Process Optimization, Chemical Characterization, and In Vitro Antioxidant, Anti-Inflammatory, and Hepatoprotective Activities

Jie Li [1,†], Hongyan Liu [1,†], Haidan Zou [1], Du Lv [2] and Heyuan Jiang [1,*]

[1] Institute of Urban Agriculture, Chinese Academy of Agricultural Sciences, National Agricultural Science and Technology Center, Chengdu 610213, China; jieli0525@163.com (J.L.)
[2] Institute of Food Processing, Guizhou Academy of Agricultural Sciences, Guiyang 550006, China
* Correspondence: jiangheyuan@caas.cn
† These authors contributed equally to this work.

Abstract

To promote the comprehensive utilization of *Gastrodia elata* (GE) resources, an efficient ultrasonic-assisted extraction (UAE) method was developed to enrich gastrodin (GAS) and phenolic constituents, which possess sedative, neuroprotective and hepatoprotective activities and exhibit promising application prospects for nutraceutical, functional food and pharmaceutical fields. Extraction parameters were optimized using a Box–Behnken design (three factors, three levels; R^2 = 0.9745, adjusted R^2 = 0.9417, lack-of-fit p = 0.5599). The optimized conditions were 65% ethanol, a liquid–solid ratio of 30 mL/g, and 60 min; the model-predicted GAS yield was 4.005 mg/g DW. UPLC-Q-TOF-MS/MS tentatively identified 32 constituents, and HPLC quantified six major compounds: parishin A (9.233 mg/g DW), parishin B (5.281 mg/g DW), GAS (4.215 mg/g DW), parishin E (3.950 mg/g DW), parishin C (1.233 mg/g DW), and p-hydroxybenzyl alcohol (0.871 mg/g DW). At 100–400 μg/mL, the extract significantly elevated SOD/GSH levels, reduced ALT/AST in a 3% ethanol-induced HepG2 hepatotoxicity model, and suppressed LPS-stimulated TNF-α/IL-6 while increasing IL-10 in RAW 264.7 macrophages (n = 3). It should be noted that anti-inflammatory assays in the present work were performed without dedicated positive reference compounds. Further investigations are required to validate bioactivities in vivo, test individual isolated constituents, and evaluate scalability together with formulation feasibility. This work provides a green, efficient strategy for the high-value utilization of GE bioactives.

Keywords: *Gastrodia elata*; gastrodin; ultrasound-assisted extraction; response surface methodology; UPLC-Q-TOF-MS/MS; in vitro bioactivity

Check for updates

Academic Editor: Chunjian Zhao

Received: 9 September 2026
Revised: 3 October 2026
Accepted: 9 October 2026
Published: 11 October 2026

Copyright: © 2026 by the authors. Licensee MDPI, Basel, Switzerland. This article is an open access article distributed under the terms and conditions of the Creative Commons Attribution (CC BY) license.

1. Introduction

Gastrodia elata (GE), a plant belonging to the genus gastrodia of the Orchidaceae family, has been traditionally used as an important Chinese herbal medicine and possesses various pharmacological activities, including sedative, anticonvulsant, antioxidant, neuroprotective, and hepatoprotective activity [1–3]. GE is widely distributed in China, Bhutan, India and Japan. Currently, it is mainly cultivated artificially. In 2019 [3,4], the National Health and Family Planning Commission of China recognized GE as a "medicinal and food homologous" plant, highlighting its great application potential in the fields of health care products,

cosmetics and functional foods [4,5]. That said, existing studies have focused mainly on the therapeutic applications of GE; however, investigating its functional constituents and health benefits from a nutritional perspective is important for advancing GE research [3]. Polyphenolic compounds, which serve as key bioactive elements in plants, have recently come under the spotlight for their promising health benefits, including powerful antioxidant, anti-inflammatory, and anti-cancer effects. As natural antioxidants, polyphenols exert significant effects in food science, pharmaceuticals, and cosmetic products [6]. Therefore, efficient extraction and utilization of the polyphenol extracts in GE is of vital importance for the development of its functional products. The dried tubers of GE are rich in the main active ingredient gastrodin (GAS), which is listed as a key index for evaluating the quality of GE in the Pharmacopoeia of China [7]. GAS, a phenolic glycoside compound, has been thoroughly examined by contemporary researchers and has been verified to possess diverse pharmacological activities. These substances demonstrate impressive neuroprotective, anti-inflammatory, antioxidant, anti-tumor, anti-depressant, and hepatoprotective properties, making them important candidates for drug development [3,7–10]. Therefore, increasing the yield of GAS in the polyphenol extract from GE is of great significance for improving the quality of products related to *Gastrodia elata*.

GE has a hard texture and dense cell walls. Common extraction methods, such as the hot reflux method and the solvent method, are extremely time-consuming. These methods may damage thermally sensitive components, consume a large amount of solvent, and are not particularly efficient in extracting active ingredients [11,12]. These factors limit the in-depth development and utilization of polyphenols in GE [11,12]. Ultrasound-assisted extraction (UAE) can disrupt plant cell walls, reduce substance transfer resistance, and accelerate solvent penetration, thereby improving the solubility and extraction efficiency of target compounds [12–14]. According to a comparison study, black tea extracted with ultrasonic assistance had about 12.93% more polyphenols than black tea extracted using the ethanol reflux method [14]. Compared with emerging extraction technologies such as supercritical fluids, microwaves, and enzymes, UAE equipment is simple in structure, operates at lower temperatures, consumes less energy, and is easy to scale up for industrial production [12,14]. It has been widely applied in the extraction of natural substances (such as polyphenols, flavonoids and polysaccharides) in a green manner [15].

Numerous previous investigations have combined response-surface-optimized UAE of *Gastrodia elata* with chemical characterization and limited biological assessment. However, many prior reports either focused primarily on extraction yield optimization with only simple biological screening assays or performed metabolomic comparison among different GE varieties without linking optimized green extraction workflows to multi-dimensional interconnected cellular bio-functional evaluation. At present, only a few studies have simultaneously integrated systematic RSM-UAE process optimization, ultra-high-performance liquid chromatography equipped with quadrupole time-of-flight mass spectrometry (UPLC-Q-TOF-MS/MS) component analysis, targeted quantitative analysis of multiple key phenolic glycoside markers, and a series of functional-related in vitro biological activity assays. All of these were accomplished under mild laboratory-scale extraction conditions using water–alcohol solutions.

Therefore, the goal of this study is to optimize the critical process factors for the ultrasound-assisted extraction of phenolic compounds from GE using Response Surface Methodology (RSM). The goal of this endeavor is to increase GAS extraction yields in the final extract. Additionally, a sophisticated analytical toolkit comprising High-Pressure Liquid Chromatography (HPLC) and UPLC-Q-TOF-MS/MS is used to perform both the qualitative and quantitative evaluation of the polyphenolic constituents present in the extract. At the same time, in vitro experiments for liver protection, antioxidant, and anti-

inflammatory effects are conducted to evaluate the biological activity of the extract in relation to GAS.

2. Materials and Methods

2.1. Materials and Chemical Reagents

GE tuber blocks were collected from Danfeng, Hanzhong, Shaanxi, China, ground into fine powder using a grinder, sieved through a 60-mesh sieve, and subsequently stored at −20 °C for subsequent experiments.

Standard samples of GAS, *p*-hydroxybenzyl alcohol, parishin A, parishin B, parishin C and parishin E were obtained from Refmedic Co., Ltd. (Chengdu, China). Methanol, ethanol, phosphoric acid, formic acid, and acetonitrile were purchased from Shanghai Macklin Biochemical Co., Ltd. (Shanghai, China). Lipopolysaccharide (LPS), cell counting kit-8 (CCK-8), minimum essential medium (MEM), and Dulbecco's modified Eagle's medium (DMEM) were obtained from Shanghai Aladdin Biochemical Technology Co., Ltd. (Shanghai, China). ELISA kits of tumor necrosis factor-α (TNF-α), interleukin-6 (IL-6), and interleukin-10 (IL-10) were obtained from Shanghai Enzyme-linked Biotechnology Co., Ltd. (Shanghai, China).

2.2. Preparation of GAS from GE by Ultrasonic-Assisted Extraction

The powder of GE (1.0 g) was mixed with an ethanol solution and then extracted using a JY 92-IIN ultrasonic processor (Ningbo Scientz Biotechnology Co., Ltd., Ningbo, China) and centrifuged (6000× *g*, 15 min). The obtained supernatant was used for further analysis and was named GE-UAE.

The effects of ethanol concentration (60–70%), liquid–solid ratio (20–40 mL/g), and extraction time (50–70 min) on the extraction rate of GAS in GE-UAE were investigated by using a single-factor experimental design (SFD), as shown in Table 1. Moreover, the findings from the one-factor test suggest that Design-Expert 13.0 software should be employed to assess how the three key variables impacted the GAS levels within the GE-UAE samples. The experimental runs and corresponding results are shown in Table 2. The GAS content (mg/g DW) was calculated as GAS content = C × V/M, where C is the GAS concentration read from the HPLC calibration curve (mg/mL), V is the final extract volume (mL), and M is the dry sample mass (g).

Table 1. Variables and levels for the Box–Behnken design of the extracts of *Gastrodia elata*.

Variable	Coded Variable	Coded Variable Level		
		−1	0	1
Ethanol concentration (%)	A	60	65	70
Solvent–solid ratio (mL/g)	B	20	30	40
Extraction time (min)	C	50	60	70

Table 2. Experimental design and response values of the BBD model.

Run	Levels of Independent Factors			GAS Content (mg/g DW)
	A (%)	B (mL/g)	C (min)	
1	65	20	50	3.596
2	60	30	50	3.615
3	65	40	70	3.648
4	60	20	60	3.646
5	60	40	60	3.703

Table 2. *Cont.*

Run	Levels of Independent Factors			GAS Content (mg/g DW)
	A (%)	B (mL/g)	C (min)	
6	65	30	60	3.900
7	70	20	60	3.541
8	60	30	70	3.510
9	70	30	70	3.454
10	65	30	60	3.886
11	65	40	50	3.659
12	65	30	60	3.955
13	65	20	70	3.560
14	70	40	60	3.643
15	65	30	60	3.917
16	65	30	60	3.847
17	70	30	50	3.560

2.3. Determination of Total Polyphenolics (TPC) and Total Flavonoid Content (TFC) in Extracts of GE-UAE

In the case of the GE-UAE, the Total Phenolic Content (TPC) was assessed by employing a refined version of the Folin–Ciocalteu spectrophotometric technique, as detailed in a recent study [15]. The TPC was reported in terms of milligrams of gallic acid equivalents per gram of dry weight (mg GAE/g DW), utilizing a gallic acid standard curve. For total flavonoid content (TFC), the AlCl3-based colorimetric method [15] was used. The TFC was quantified in milligrams of rutin equivalents per gram of dry weight (mg RE/g DW) and calculated using the rutin calibration curve.

2.4. Identification of Phenolic Compounds in GE-UAE by UPLC-Q-TOF-MS/MS

An Agilent 6545 LC/Q-TOF mass spectrometer (Agilent Technologies, Santa Clara, CA, USA) was used for the UPLC-Q-TOF-MS/MS analysis. Data processing was carried out using MassHunter software (version 11.0, Agilent Technologies, Santa Clara, CA, USA). The chromatographic column used was Eclipse Plus C18 RRHD, with a size of 2.1 × 50 mm and a particle size of 1.8 micrometers, maintained at a constant temperature of 30 degrees Celsius. The mobile phase was formed by mixing solvent A (water) and solvent B (methanol), and the injection volume was fixed at 3 microliters. Over the course of 16 min, each sample was flushed out at a constant rate of 0.4 mL per minute. The characteristic of the rinsing process was a gradually changing concentration gradient: within the time period of 0 to 1 min, the concentration started to decrease from 90% A and reached 45% A at 1 to 3 min. Subsequently, the concentration continued to decline, reaching 40% A at 3 to 7 min and 10% A at 7 to 11 min. During the period of 11 to 13 min, the concentration remained at 10%. After that, the concentration gradient was reversed from 10% to 90% A over 13–16 min for column re-equilibration. The mass spectrometer was set up using the negative ion mode with a voltage of 2.0 kilovolts for the electrospray ion source. All the sampling cone voltages were locked at 40.0 kilovolts.

2.5. Quantification of Major Phenolic Compounds in GE-UAE by HPLC

When measuring the primary phenolic compounds in GE-UAE, an Agilent 1260 II high-performance liquid chromatography system (Agilent Technologies, Santa Clara, CA, USA) was employed. This method was meticulously developed by previous researchers. To analyze the samples, we used the Agilent Zorbax SB-C18 chromatographic column (Agilent Technologies, Santa Clara, CA, USA), which has a size of 250 mm × 4.6 mm and a particle size of 5 micrometers. The mobile phase for the separation was a 0.05% (v/v)

solution of phosphoric acid, while acetonitrile served as solvent B. Gradient elution was employed as follows: 0–5 min, 2% A; 5–20 min, 2–30% A; 20–25 min, 30–2% A; detection wavelength: 220 nm; volume flow rate: 1.0 mL/min; column temperature: 25 °C; injection volume: 10 μL. To quantitatively investigate the phenolic compounds in the extract, six standards were used, including gastrodin, *p*-hydroxybenzyl alcohol, parishin A, parishin B, parishin C, and parishin E.

2.6. Evaluation of the Hepatoprotective Activity and Antioxidant Activity of GAS and GE-UAE

A modified approach was used to examine the hepatoprotective activity [16]. A HepG2 cell suspension at 5×10^4 cells/mL was used to inoculate 96-well plates. Each well received 100 μL of the cell suspension, which was then grown for 24 h. After the cells attached to the wall, 100 μL of alcohol-containing cell culture media (0.5%, 1%, 2%, 3%, 4%, 5%, and 6%, respectively) was added to each well. After the supernatant was completely absorbed, the cells were further cultured for 24 h. Subsequently, the cell viability was evaluated using the CCK-8 assay.

During the inoculation process, we used a HepG2 cell suspension with a concentration of 1×10^5 cells per well for inoculation. The cells were evenly spread out in a 24-well plate, with 1 milliliter of the cell suspension added to each well. After 24 h of cultivation, the experimental setup was divided into four groups: a control group, a model group, a treatment group, and a positive control group. To ensure the reliability of the statistics, three replicate wells were carefully set up for each group. The culture medium was added to both the control group and the model group. The positive control group was treated with bifendate (400 μg/mL), while the treatment groups were GE-UAE (50–400 μg/mL) and GAS (50–400 μg/mL). The plates were incubated at 37 °C in a humidified 5% CO_2 atmosphere for 24 h, after which the culture supernatant was collected. In the control group, a mere 1 milliliter of culture medium was poured into each container. In the model group, positive group and administration group, 1 mL of 3% alcohol culture medium was added to each well. The samples were incubated at 37 °C for 24 h, after which the culture supernatant was collected. Subsequently, the concentrations of alanine aminotransferase (ALT), aspartate aminotransferase (AST), malondialdehyde (MDA), superoxide dismutase (SOD), and glutathione (GSH) in the supernatant were determined using commercial assay kits according to the manufacturer's instructions.

2.7. Evaluation of the Anti-Inflammatory Activity of GAS and GE-UAE

The anti-inflammatory assay was performed following a modified protocol by [15]. RAW 264.7 cells were seeded into 96-well plates at a density of 5×10^4 cells/well and cultured for 24 h at 37 °C in a humidified 5% CO_2 incubator. The supernatant was discarded, then GE-UAE (50–400 μg/mL) and GAS (50–400 μg/mL) were added, and the complete medium was used as the blank control. After incubation for 24 h, the cell viability was determined by the CCK8 method.

Utilizing the protocol from the last study, RAW 264.7 cells were grown at a density of 1×10^5 cells per well in 24-well plates and allowed to culture for a period of 24 h. Following this, the supernatant from each well was carefully discarded. To the wells, except for the control group, LPS (at a concentration of 1 μg/mL) was then introduced, and the mixture was once again incubated for an additional 24 h. Samples were subsequently added, and incubation was carried out for 24 h. The supernatant was collected for determination of IL-6, IL-10, and TNF-α concentrations.

2.8. Statistical Analysis

Statistical significance was evaluated via one-way ANOVA and Student's *t*-tests, with a threshold set at $p < 0.05$. A software suite including Design Expert 11, IBM SPSS Statistics

(version 27.0, IBM Corp., Armonk, NY, USA), and Origin 2022 was utilized in this analysis. The findings were presented as means ± standard deviations (n = 3).

3. Results and Discussion

3.1. Optimal Extraction Conditions of UAE

3.1.1. Optimal Conditions of UAE

Ultrasonic-assisted extraction (UAE) is a high-speed, eco-friendly technique with remarkable effects. Typically, factors like the liquid-to-solid ratio, the strength of the solvent, the intensity of the extraction process, and the duration of the ultrasound exposure all have significant impacts on the performance of the UAE method.

Water molecules can promote the expansion of plant substances, while ethanol can disrupt the binding between solutes and the plant structure [17]. The chart in Figure 1A shows that when the ethanol concentration increases from 60% to a 65% mixture, the total amount of extracted GAS shows a significant increase. However, when the ethanol concentration further increases from 65% to 80%, the yield significantly decreases. The current trend can likely be explained by the impact of ethanol concentration. If the concentration is insufficient, the process through plant cells will be affected. Additionally, excessive ethanol will change the polarity of the solvent, which is not ideal for dissolving polar polyphenols [18,19]. The research indicates that competitive intermolecular interactions exist among ethanol, water, and polyphenol molecules [20,21]. These findings align with earlier research that used ultrasound to extract polyphenols from the Areca nut [21]. The liquid-to-solid ratio is a crucial extraction parameter, as it affects the concentration gradient between the solid and liquid phases [17,22]. Generally, ethanol can effectively solubilize and extract polyphenols from plant matrices and is an important solvent that affects the extraction rate [17,23]. Figure 1B shows that the yield of GAS in the extract first increased and subsequently fell when the liquid–solid ratio increased from 10:1 to 50:1 mL/g. The highest polyphenol yield is 3.92 mg/g when the liquid–solid ratio is 30 mL/g. The diffusion of components within plant tissues may benefit from an increase in the contact area of the solvent [17,18]. On the other hand, an excessively high liquid-to-solid ratio may restrict the ultrasound's depth, which would reduce the extraction process's overall effectiveness [17,24]. Studies on the extraction of polyphenols from Japanese honeysuckle leaves have confirmed these results [18]. The significant influence that the length of ultrasonic exposure has on the ultimate GAS output is shown in Figure 1C. The content of GAS gradually increased with extended ultrasonic time until it reached 60 min, but further increases in the ultrasonic time led to a decrease in the content of GAS. Extending the ultrasonic time is beneficial for the release of active ingredients [18]. However, if the ultrasonic time is too long, it may lead to the decomposition of active ingredients due to the enhanced thermal and mechanical effects of ultrasound [17,25]. This outcome is in line with studies that extracted polyphenols from *Vaccinium dunalianum* leaves using an ultrasonic-assisted method [26]. The impact of changing ultrasonic power on the GAS yield from GE is shown in Figure 1D. The GAS concentration continued to rise as the ultrasonic power increased, peaking at 400 W. Beyond this power, the content of GAS remained relatively stable. Generally, as the ultrasonic power increases, the cavitation effect gradually increases, thereby enhancing mass transfer and cell fragmentation caused by bubble collapse, and the active ingredients are easier to release into the solvent [17,18]. However, if the power is too high, it could harm the structure of cells' active components, which would lower the extraction rate of GAS [25]. The findings of research employing ultrasound-assisted polyphenol extraction from pecan "Shaoxing" green husk are in line with this pattern [27].

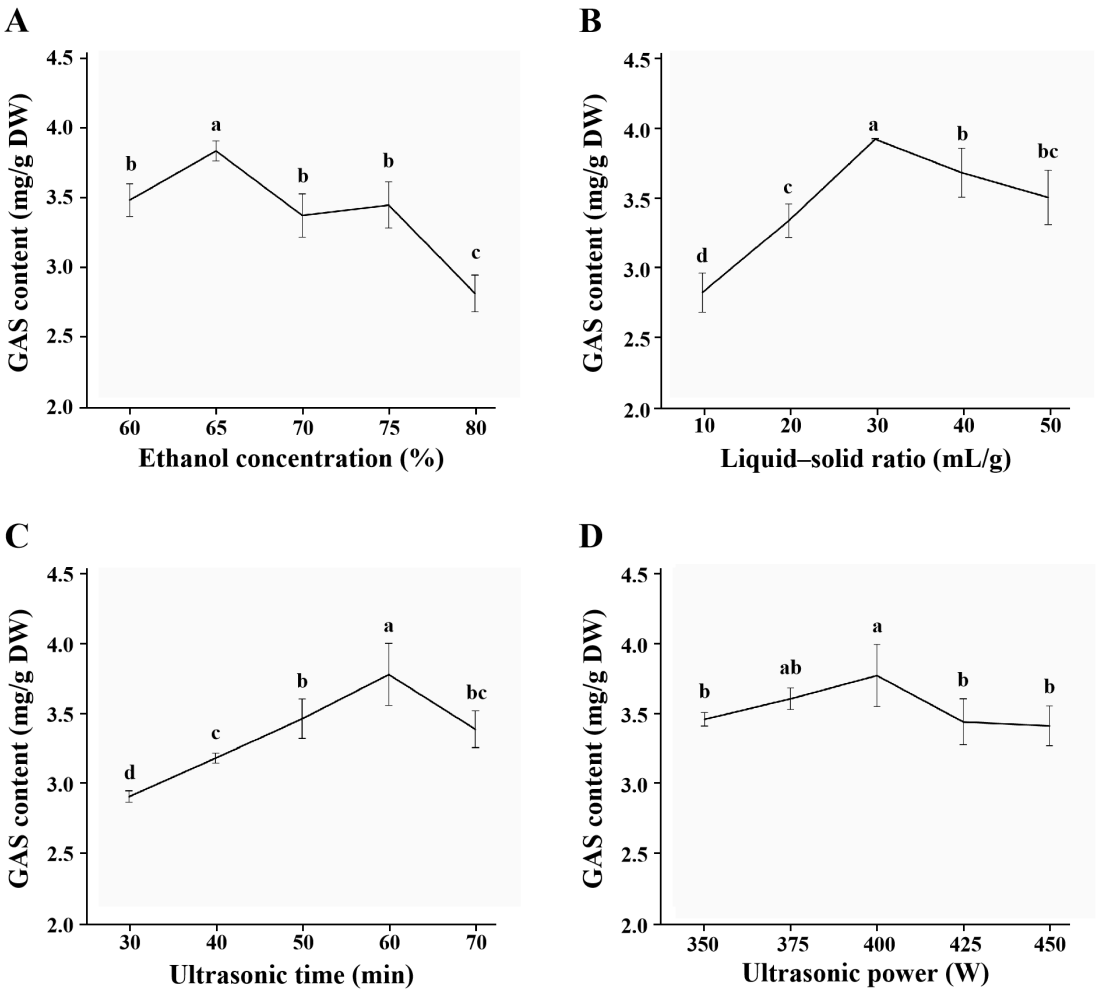


Figure 1. Optimal conditions from the single-factor experiment. Effects of ethanol concentration (**A**), liquid-to-solid ratio (**B**), ultrasonic time (**C**), and ultrasonic power (**D**) on the yield of GAS extracted from GE by ultrasonic-assisted extraction. Different letters (a–d) indicate significant differences at $p < 0.05$ as determined by ANOVA.

3.1.2. Optimal Conditions from the Box–Behnken Design (BBD)

The response surface optimization (RSM) method can evaluate the interactions among multiple parameters [25]. Based on the results of single-factor experiments, three variables—liquid–solid ratio, ethanol concentration, and ultrasonic time—were selected as the independent factors for response surface optimization. In the response surface method, a complete block design (BBD) experiment was used to study the relationship between these variables and the response, with the yield of GAS in the polyphenol extract as the response variable. Through the 17 experiments generated by the BBD (including 12 interaction experiments and five central experiments), a regression equation was obtained. Table 1 summarizes the results of these studies.

$$Y = 3.901 - 0.0345A + 0.03875B - 0.03225C + 0.01125AB - 0.00025AC + 0.00625BC - 0.174375A^2 - 0.093375B^2 - 0.191875C^2$$

where A is the ethanol concentration (%), B is the liquid–solid ratio (mL/g), C is the ultrasonic time (min), and Y is the GAS yield.

Table 3 summarizes the information from the ANOVA analysis. This model is statistically significant because its simulated p-value is less than 0.0001 [15,28]. The generated model fits well, as evidenced by the misfitting term's p-value of 0.5599 [15,29]. The R^2

is 0.9745 and the adjusted R^2 is 0.9417, indicating that the model can be used for further analysis and prediction. The linear parameters (A, B, and C) reached the significant level, and the quadratic parameters (A^2, B^2, and C^2) reached the highly significant level. The comprehensive analysis showed that the regression model is reasonable.

Table 3. Analysis of variance (ANOVA) results of the model.

Source	Sum of Squares	DF	Mean Square	F-Value	*p*-Value
Model	0.3840	9	0.0427	29.72	<0.0001 **
A	0.0095	1	0.0095	6.63	0.0367 *
B	0.0120	1	0.0120	8.37	0.0232 *
C	0.0083	1	0.0083	5.80	0.0469 *
AB	0.0005	1	0.0005	0.3527	0.5713
AC	2.5×10^{-7}	1	2.5×10^{-7}	0.0002	0.9898
BC	0.0002	1	0.0002	0.1088	0.7511
A^2	0.1280	1	0.1280	89.19	<0.0001 **
B^2	0.0367	1	0.0367	25.57	0.0015 **
C^2	0.1550	1	0.1550	107.99	<0.0001 **
Residual	0.0100	7	0.0014		
Lack of Fit	0.0037	3	0.0012	0.7886	0.5599
Pure Error	0.0063	4	0.0016		
Cor Total	0.3940	16			
R^2	0.9745				
Adjusted R^2	0.9417				
Predicted R^2	0.8233				

* $p < 0.05$ indicates statistical significance; ** $p < 0.01$ indicates high statistical significance.

The response surface and contour plots in Figure 2 illustrate how each element affects GAS yield and how any two factors interact. The interaction impact between factors is more visible in a 3D surface plot that is steeper [17]. The response surface plots of the two-by-two interactions of ethanol concentration, material–liquid ratio, and extraction time in earlier research showed a hill-like form, suggesting that these three variables had a significant impact on the extracted content of GAS. The contour plots showed elliptical contour lines indicating significant interactions between the two factors. The graphs of ethanol concentration versus material–liquid ratio and extraction time versus material–liquid ratio presented an elliptical shape [21,26]. The model study projected the following ideal extraction process parameters: ethanol concentration of 64.26%, solid–liquid ratio of 31.87 mL/g, and extraction time of 59.58 min. In practical applications, the best extraction procedure found was as follows: ethanol concentration of 65%, solid–liquid ratio of 30 mL/g, and extraction time of 60 min. Under the rounded practical UAE condition, the model-predicted GAS yield was 4.005 mg/g DW, and experimental validation gave 4.215 mg/g DW, with a relative deviation of 5.24%, indicating good fitness of the Box–Behnken model. The content of TPC was 5.862 mg GAE/g DW and the content of TFC was 2.255 mg RE/g DW when the validation experiment was repeated under these extraction circumstances.

To further evaluate the performance of the optimized UAE strategy, its extraction efficiency and green-related attributes were compared with two representative conventional extraction approaches, heating reflux and static maceration, based on previously published comparable literature data (Table 4). In this study, 65% aqueous ethanol was selected as the extraction solvent based on green chemistry considerations. Compared with toxic organic solvents such as methanol and chloroform, aqueous ethanol mixtures exhibit low acute toxicity. At a laboratory scale, ethanol can be readily recovered via rotary evaporation with acceptable recyclability (>90% recovery rate under typical lab conditions). As summarized in Table 4, our optimized UAE shortens the extraction duration substantially compared

with heating reflux and static maceration. Although ultrasonic treatment consumes electric energy for cavitation generation, UAE avoids prolonged continuous heating required by reflux extraction, leading to reduced overall energy demand under laboratory-scale operation. It should be emphasized that the above-mentioned green-related assessments are semi-quantitative estimations obtained under lab-scale experimental settings. Formal life-cycle assessment would be essential for further industrial-scale implementation of this extraction workflow.

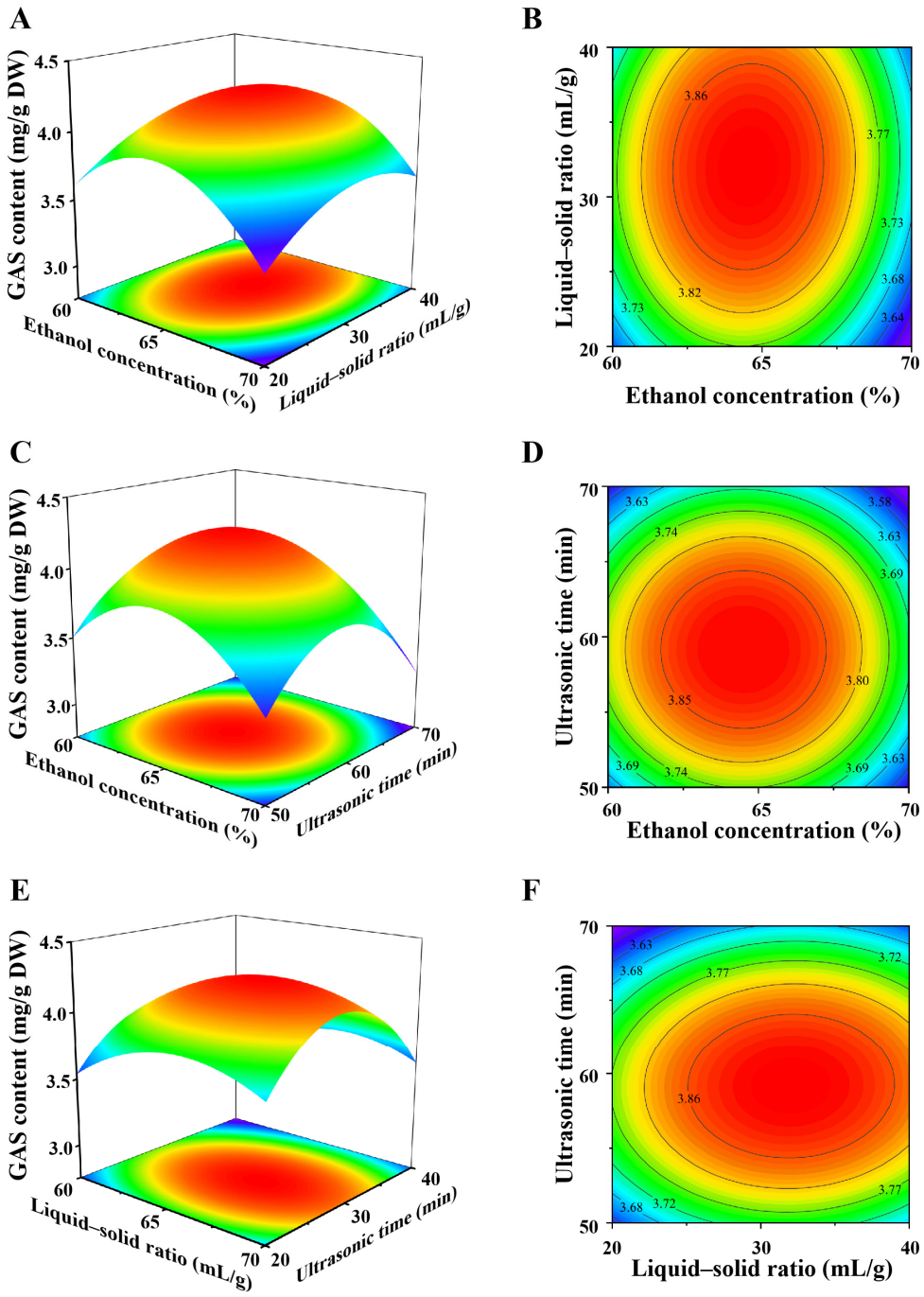


Figure 2. 2D/3D plots of the fitted model. Three-dimensional response surface plots (**A**,**C**,**E**) and two-dimensional contour plots (**B**,**D**,**F**) of ultrasonic-assisted extraction. (**A**–**F**) represent the interactions among ethanol concentration, ultrasonic time and liquid–solid ratio, respectively. The color gradient in the surface and contour plots corresponds to the GAS content (mg/g DW): blue indicates the lowest fitted value, while red indicates the highest fitted value at the response peak.

Table 4. Comparison of extraction performance between the optimized UAE procedure and conventional extraction techniques for GAS from GE.

Extraction Method	Extraction Solvent	Liquid–Solid Ratio (mL/g)	Extraction Time	Gastrodin Yield (mg/g DW)	Relative Solvent Consumption	Relative Energy Input	Reference
Present optimized UAE	65% aqueous ethanol	30	60 min	4.215	Low	Low	This work
Heating reflux	70% aqueous ethanol	30	120 min	3.42	Moderate	High	[30,31]
Static maceration	70% aqueous ethanol	30	48 h	2.87	Moderate-high	Very low	[31]

Yield and operational parameters for conventional extraction approaches were compiled from the peer-reviewed comparable literature under aqueous ethanol extraction conditions. Raw material botanical origins and batches may differ from the sample used in the present study. Relative solvent consumption and relative energy input represent semi-quantitative laboratory-scale estimations instead of absolute calorimetric measurements.

3.2. Identification and Quantification of Major Compounds in GE-UAE

The total ion chromatogram (TIC) of GE-UAE in negative mode was obtained by UPLC-Q-TOF-MS/MS. Based on previous literature [4,32] and the Mass Bank database, 32 compounds were preliminarily identified in GE-UAE. Their retention times, molecular formulae, calculated m/z and observed m/z are listed in Table 5. These 32 compounds include nine glycosides, eight phenolic and aromatic derivatives, seven organic acids, three amino acids, three nucleotides/nucleosides, one purine base, and one carbohydrate. Based on prior research, databases, and multiple reliable standards, these substances were tentatively recognized as malic acid, L-pyroglutamic acid, uridine 5′-monophosphate, fumaric acid, sucrose, 1-β-D-ribofuranosyl uracil, L-tyrosine, citric acid, adenine, L-leucine, β-D-glucopyranoside, 4-hydroxy-2,6-dimethoxyphenyl, GAS, 3,4-dihydroxybe nzaldehyde, catalpol, sorbic acid, *p*-hydroxybenzaldehyde, L-aspartic acid, dimethyl phthalate, trans-aconitic acid, parishin E, 4-hydroxybenzoic acid, aucubin, ethyl gallate, benzoic acid, verbascoside, parishin C, parishin B, *p*-hydroxylbenzyl alcohol, parishin A, ethyl ferulate, and phenyl benzoate. Furthermore, these compounds have also been found to exist in different varieties of GE [3,4,32–37].

Furthermore, high-performance liquid chromatography was used to identify the primary phenolic compounds in GE-UAE. High-performance liquid chromatograms of the diluted GE-UAE and the mixed standard are displayed in Figure 3. The calibration information for the six chemicals and their concentrations in GE-UAE is compiled in Table 6. As shown in Table 6, the content levels of the six main components in GE-UAE are in the following order: parishin A > parishin B > GAS > parishin E > parishin C > *p*-hydroxybenzyl alcohol. This indicates that GE-UAE contains a relatively high amount of tuberine and parishin compounds. It has been reported that Parishin-type compounds have neuroprotective, anti-inflammatory, and liver-protective activities, while organic acids contribute to the antioxidant effect [3,4]. Additionally, HPLC analysis revealed a significantly lower total phenol level than the Folin–Ciocalteu colorimetric method, which is consistent with earlier research. This could be because the Folin–Ciocalteu colorimetric method's accuracy could be impacted by the presence of amino acids, reducing sugars, and ascorbic acid in the crude extract, whereas high-performance liquid chromatography analysis exclusively concentrated on the six phenolic chemicals [15,38].

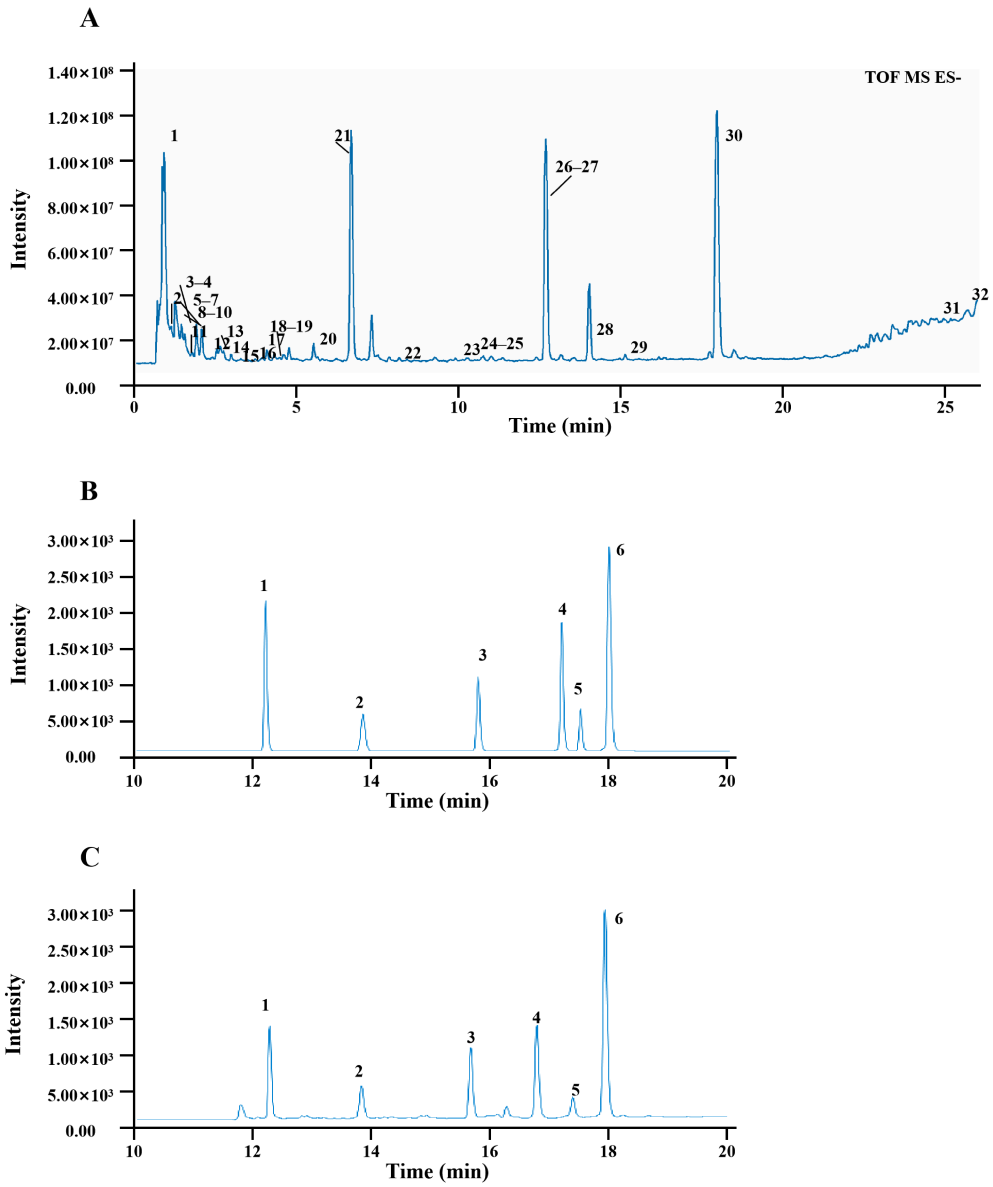


Figure 3. UPLC-Q-TOF-MS/MS total ion chromatography (TIC) of GE-UAE (**A**). HPLC-UV plots of mixed standards (**B**) and GE-UAE (**C**). The numbered peak labels in panels (**B**) and (**C**) correspond to the six target phenolic constituents identified in this study: 1 = gastrodin, 2 = *p*-hydroxybenzyl alcohol, 3 = parishin E, 4 = parishin B, 5 = parishin C, 6 = parishin A.

Table 5. Tentative identification of compounds in GE-UAE by UPLC-ESI-Q-TOF-MS/MS.

	RT	Compound	Molecular Formula	CAS	Mass	Observed [MH]-
1	0.971	Malic acid	$C_4H_6O_5$	6915-15-7	134.0212	133.0137
2	1.093	L-Pyroglutamic acid	$C_5H_7NO_3$	98-79-3	129.0425	128.0352
3	1.312	Uridine 5′-monophosphate	$C_9H_{13}N_2O_9P$	58-97-9	324.0357	323.0284
4	1.320	Fumaric acid	$C_4H_4O_4$	110-17-8	116.0106	175.0244
5	1.434	Sucrose	$C_{12}H_{22}O_{11}$	57-50-1	342.1172	341.1087
6	1.448	1-β-D-Ribofuranosyl uracil	$C_9H_{12}N_2O_6$	58-96-8	244.0692	243.0621
7	1.457	L-Tyrosine	$C_9H_{11}NO_3$	60-18-4	181.0736	180.0661
8	1.516	Citric acid	$C_6H_8O_7$	77-92-9	192.0268	191.0195
9	1.539	Adenine	$C_5H_5N_5$	73-24-5	135.0547	134.0474
10	1.584	L-Leucine	$C_6H_{13}NO_2$	61-90-5	131.0945	130.0872
11	1.729	*β*-D-Glucopyranoside, 4-Hydroxy-2,6-dimethoxyphenyl	$C_{14}H_{20}O_9$	121748-12-7	332.11	331.1026
12	2.221	Gastrodin	$C_{13}H_{18}O_7$	138-52-3	286.1052	285.0981

Table 5. *Cont.*

	RT	Compound	Molecular Formula	CAS	Mass	Observed [MH]-
13	2.661	3,4-Dihydroxybe nzaldehyde	$C_7H_6O_3$	139-85-5	138.1200	137.0245
14	3.161	Catalpol	$C_{15}H_{22}O_{10}$	2415-24-9	362.1212	361.1141
15	3.630	Sorbic acid	$C_6H_8O_2$	110-44-1	112.0525	157.0507
16	4.093	*p*-Hydroxybenzaldehyde	$C_7H_6O_2$	123-08-0	120.0437	119.0364
17	4.365	L-Aspartic acid	$C_4H_7NO_4$	56-84-8	133.0376	132.0307
18	4.570	Dimethyl phthalate	$C_{10}H_{10}O_4$	131-11-3	194.0579	193.0506
19	4.629	Trans-aconitic acid	$C_6H_6O_6$	4023-65-8	174.0163	173.009
20	5.897	Parishin E	$C_{19}H_{24}O_{13}$	952068-57-4	460.390	459.387
21	6.516	4-Hydroxybenzoic acid	$C_7H_6O_3$	99-67-7	138.0316	137.0242
22	8.411	Aucubin	$C_{15}H_{22}O_9$	479-98-1	346.1266	391.1249
23	10.274	Ethyl gallate	$C_9H_{10}O_5$	831-61-8	198.0526	197.0453
24	11.266	Benzoic acid	$C_7H_6O_2$	65-85-0	122.0369	121.0296
25	11.707	Adenosine	$C_{10}H_{13}N_5O_4$	58-61-7	267.0968	266.0894
26	12.744	Verbascoside	$C_{29}H_{36}O_{15}$	61276-17-3	624.2053	669.2032
27	12.948	Parishin C	$C_{32}H_{40}O_{19}$	174972-80-6	728.2156	727.2080
28	14.395	Parishin B	$C_{32}H_{40}O_{19}$	174972-79-3	728.2153	727.2070
29	15.358	*p*-Hydroxylbenzyl alcohol	$C_7H_8O_2$	623-05-2	124.0524	123.0451
30	18.184	Parishin A	$C_{45}H_{56}O_{25}$	62499-28-9	996.3107	995.3032
31	25.094	Ethyl ferulate	$C_{12}H_{14}O_4$	4046-02-0	222.0893	221.0819
32	26.276	Phenyl benzoate	$C_{13}H_{10}O_2$	93-99-2	198.0677	197.0604

Table 6. Contents of major phenolic compounds in GE-UAE.

Compounds	Regression Equation	R^2	Retention Time (min)	Linear Range (μg/mL)	GE-UAE (mg/g DW)
Gastrodin	y = 17.4915x − 15.6818	0.99978	12.153	30.0–210.0	4.215 ± 0.036
p-Hydroxybenzyl alcohol	y = 53.3230x + 10.7302	0.99933	13.8	10.0–50.0	0.871 ± 0.008
Parishin E	y = 25.6986x + 26.3247	0.99949	15.748	50.0–250.0	3.950 ± 0.055
Parishin B	y = 23.6370x − 7.9128	0.99988	17.163	30.0–210.0	5.281 ± 0.051
Parishin C	y = 22.6273x + 6.5790	0.99964	17.481	5.0–60.0	1.233 ± 0.043
Parishin A	y = 30.3339x + 0.9244	0.99906	17.963	50.0–350.0	9.233 ± 0.170

3.3. Evaluation of the Hepatoprotective Activity of GAS and GE-UAE

Using the CCK-8 assay, the effects of varying GAS and GE-UAE concentrations on HepG2 cell viability were assessed; the findings are displayed in Figure 4. GAS and GE-UAE did not significantly harm HepG2 cells at concentrations between 50 and 400 μg/mL as compared to the blank control group. Even at the greatest dose of 400 μg/mL, the positive medication did not significantly harm the cells.

The in vitro hepatoprotective effects of GAS and GE-UAE were compared using an alcoholic HepG2 cell model. The impact of various ethanol concentrations on cell viability was assessed in order to ascertain the concentration of action of ethanol-induced liver damage. As shown in Figure 4A, different concentrations of alcohol affected cell viability to different degrees; as the alcohol concentration increased, the cell survival rate gradually decreased. At the alcohol concentrations of 0.5%, 1%, 2%, 3%, 4%, 5%, and 6%, the survival rates were 85.43%, 78.02%, 68.04%, 50.93%, 47.48%, 31.08%, and 29.38%, respectively; therefore, the 3% concentration of alcohol was chosen to induce the establishment of an alcoholic liver disease (ALD) model of HepG2. Furthermore, the cell viability after treating the liver injury cell model with different concentrations of GAS and GE-UAE (50–400 μg/mL) was investigated. As shown in Figure 4B, the modest doses of GAS (50 μg/mL) and GE-UAE (50–100 μg/mL) had no restorative effect on HepG2 cell activity compared to the model group. HepG2 cell activity differed significantly from the model group when the dose of GAS rose from 100 μg/mL to 400 μg/mL. When the concentration of GE-UAE was between 200 and 400 μg/mL, there was also a significant difference in the cell activity of HepG2 compared with the model group. Importantly, the high doses

(400 μg/mL) of GAS and GE-UAE had a stronger restorative effect on the cell activity of HepG2 than the positive group, indicating that both GAS and GE-UAE have good abilities to protect against liver cell damage.

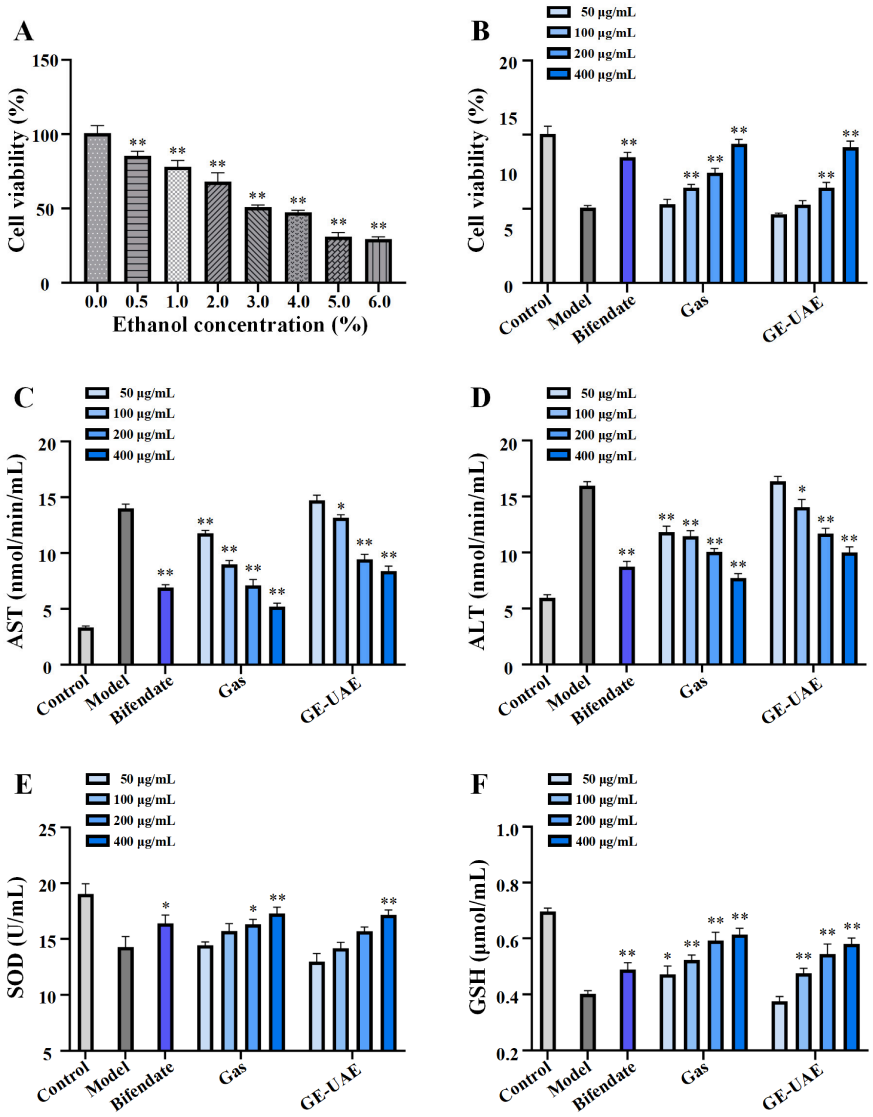


Figure 4. The hepatoprotective and antioxidant activities of GAS and GE-UAE. The effects of different concentrations of alcohol on cell viability (**A**); the effects of different concentrations of GAS and GE-UAE on the cell viability of HepG2 (**B**); the effects of different concentrations of GAS and GE-UAE on AST and ALT production (**C**,**D**); the effects of different doses of GAS and GE-UAE on the release of SOD and GSH content by HepG2 cells (**E**,**F**). Cell viability is expressed as a percentage relative to the untreated control group (set as 100%). The error bars are standard deviations; significant differences between samples are shown by * $p < 0.05$ and ** $p < 0.01$.

Aspartate aminotransferase (AST) and alanine aminotransferase (ALT) are crucial markers of hepatocyte health. Hepatocyte injury is usually characterized by the release levels of ALT and AST [39,40]. Research has demonstrated that GAS therapy can have a hepatoprotective impact on animals with alcoholic liver injury by lowering the activity of ALT and AST in the serum. HepG2 cells stimulated with 3% ethanol had much higher levels of AST and ALT in the model group's culture medium supernatant, as seen in Figure 4C,D. However, treatment with GAS and GE-UAE significantly reduced AST and ALT levels, showing a similar trend to the positive control (bifendate), suggesting that GAS and GE-UAE have outstanding potential in protecting hepatocytes. Moreover, GAS

was more effective than GE-UAE. The above results indicate that both GAS and GE-UAE have some ability to protect against hepatocyte injury. Studies have shown that GAS can protect liver cells from apoptosis by regulating multiple signaling pathways, promoting the expression of various endogenous antioxidants, and reducing the expression of inflammatory factors. As a result, it can inhibit oxidative stress and inflammation in various liver injury models [10]. For instance, Zhang found that GAS decreased the activity of ALT and AST in mice with ethanol-induced alcoholic liver disease within the dosage range of 50–100 mg/kg via activating the Nrf2 signaling route and blocking the TLR4/NF-κB signaling network [41]. Furthermore, studies have shown that parishin A can improve neurological and psychiatric disorders related to liver dysfunction by increasing the activity of EAAT3 in the intestinal microbiota [42]. On the other hand, based on the results of compound identification, GE-UAE contains organic acids, which can undergo esterification reactions with alcohols to form esters. These organic acids and their esters have pharmacological effects such as liver protection and antioxidation [37].

3.4. Evaluation of the Antioxidant Activity of GAS and GE-UAE

GAS exhibits significant antioxidant properties both in vitro and in vivo [8]. Additionally, GAS inhibits lead-induced oxidative stress by regulating the glutathione, thioredoxin (Trx), and Nrf2 antioxidant systems, and supplementing GAS can increase the activation of SOD, GPx, HO-1, and NQO1 in the kidneys. One study found that after treatment with GAS, the content of MDA in the liver of mice with alcoholic liver injury was reduced, while the activities of SOD, GPx, and CAT increased [43]. Ahmad et al. found that within the concentration range of 10–50 mg/kg, GAS exhibited antioxidant effects on non-alcoholic fatty liver disease in zebrafish induced by a high-cholesterol diet and reduced the levels of ROS and MDA [9]. However, the antioxidant activity of GE-UAE remains unclear.

Excessive ethanol metabolism in hepatocytes generates a large number of free radicals, which rapidly combine with intracellular ethanol or iron atoms to form reactive metabolites, ultimately causing oxidative stress [44–46]. Reducing oxidative stress is mostly dependent on intracellular antioxidants like SOD and GSH, which scavenge excess free radicals. SOD's primary job is to change superoxide into water and hydrogen peroxide [47]. GSH is one of the major endogenous antioxidants produced by cells and can be directly involved in the neutralization of free radicals and reactive oxygen compounds [48]. As shown in Figure 4E,F, compared with the blank group, both the SOD and GSH contents of the model group were significantly lower than those of the blank group. Compared with the model group, both the positive and sample groups had significantly increased SOD and GSH contents, and both showed certain dose effects. Phenolic compounds with a benzene ring structure exhibit remarkable antioxidant properties due to the hydroxyl and aldehyde groups present on the benzene ring [37]. Furthermore, the dimer and trimer compounds derived from *p*-hydroxybenzyl alcohol through condensation reactions in GE-UAE exhibit stronger activity in the cell model compared to *p*-hydroxybenzyl alcohol and GAS [49]. Therefore, it is likely that the synergistic effect of multiple compounds in GE-UAE contributes to its superior antioxidant activity compared to GAS.

3.5. Evaluation of the Anti-Inflammatory Activity of GAS and GE-UAE

It has been demonstrated that GAS has strong anti-inflammatory properties. In the LPS-induced BV2 cell inflammation model, it can reduce inflammation by controlling the expression of IL-1β, IL-6, IL-23, TNF-α, and NO [7,50]. Furthermore, GAS can alleviate Pb-induced renal inflammation by lowering TNF-α and IL-6 levels [43]. GAS also suppresses LPS-induced macrophage inflammatory responses and pro-inflammatory cytokine release in the atherosclerotic mouse model via downregulating the NF-κB pathway [51]. Never-

theless, it is currently unknown if polyphenol extracts from GE have anti-inflammatory properties in vitro. Thus, the anti-inflammatory properties of polyphenol extracts derived from ultrasonic extraction were investigated and contrasted with GAS in vitro.

The effects of GAS and GE-UAE on RAW 264.7 macrophage cell viability are displayed in Figure 5A. The findings showed that within the concentration range of 50–400 micrograms per milliliter, no samples showed any cytotoxic effects on RAW 264.7 macrophages. IL-10 is a crucial anti-inflammatory cytokine, while TNF-α and IL-6 are significant pro-inflammatory mediators. As illustrated in Figure 5B–D, the expression levels of TNF-α and IL-6 in the model group were significantly higher than those in the blank group, while the expression level of IL-10 was significantly lower. Following the intervention with GAS and GE-UAE, the levels of TNF-α and IL-6 were significantly reduced, while the level of the anti-inflammatory factor IL-10 was significantly increased. The findings showed that GAS and GE-UAE may suppress the inflammatory response by increasing the release of IL-10 and decreasing TNF-α and IL-6. Research has demonstrated that GE has anti-inflammatory and antioxidant benefits by controlling energy and purine metabolism [37]. In addition, the parishin compounds (especially parishin C) in GE-UAE have also been reported to inhibit the release of oxidative stress and pro-inflammatory factors [49]. It is worth noting that in the current detection scheme, no synthetic anti-inflammatory positive control compounds (such as dexamethasone or indomethacin) were included. Subsequent pharmacodynamic studies will implement a benchmark pharmacodynamic test, including positive controls.

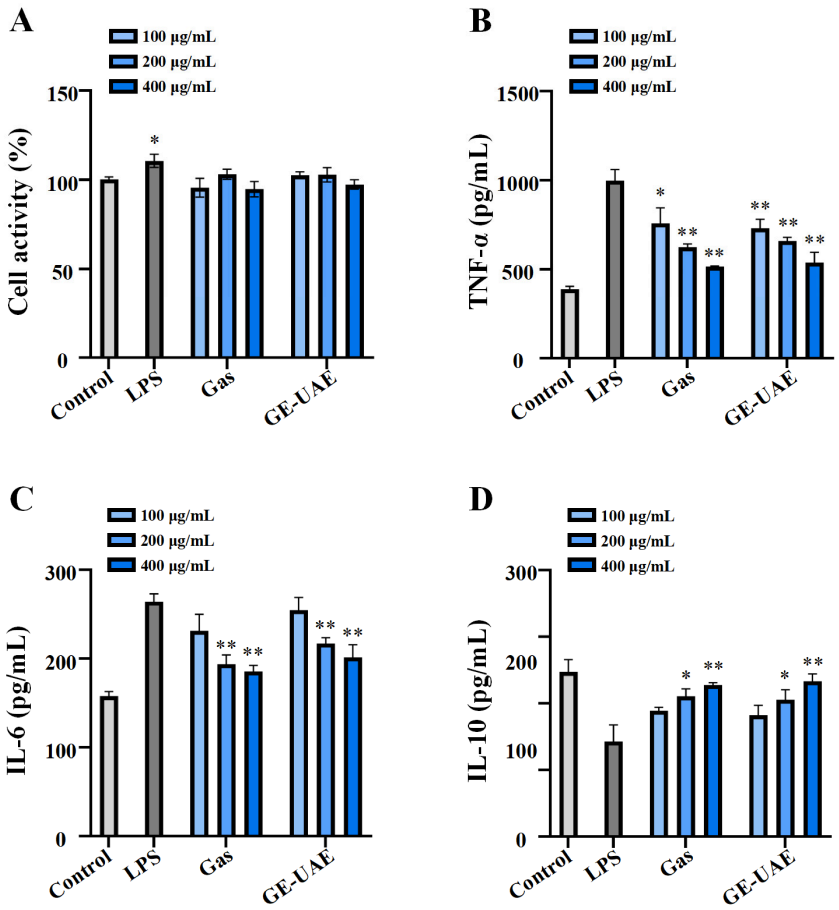


Figure 5. The anti-inflammatory activity of GAS and GE-UAE. The effects of different doses of GAS and GE-UAE on the cell viability of Raw 264.7 (**A**); the effects of different doses of GAS and GE-UAE on the production levels of TNF-α, IL-6 and IL-10 (**B**–**D**). Cell viability is expressed as a percentage relative to the untreated control group (set as 100%). The error bars are standard deviations; significant differences between samples and control are shown by * $p < 0.05$ and ** $p < 0.01$.

4. Conclusions

By applying RSM to optimize the ultrasound-assisted extraction (UAE) of phenolic components from GE, this study developed an efficient UAE method under the tested laboratory conditions that provides a potentially greener alternative to conventional solvent extraction. UPLC-Q-TOF-MS/MS and HPLC were applied for qualitative and quantitative analysis of extract constituents. Furthermore, the hepatoprotective, antioxidant, and anti-inflammatory activities of GE-UAE were evaluated via in vitro cell models and compared with pure gastrodin (GAS). The findings demonstrated that bioactive phenolic components from GE can be effectively recovered using this optimized UAE approach. GE-UAE contains abundant phenolic compounds that exert notable cellular anti-inflammatory, antioxidant, and hepatoprotective effects. These results provide theoretical foundations and technical support for the comprehensive development and application of GE in functional food and pharmaceutical fields. This cost-effective and environmentally friendly extraction strategy also offers a reference for harvesting bioactive ingredients from other medicinal plants.

Compared with previous investigations on *Gastrodia elata* extraction and bioactivity, the present work makes several distinct incremental contributions. Rather than focusing merely on extraction parameter optimization paired with rudimentary biological readouts, this study couples a fully optimized, room-temperature mild 65% aqueous ethanol UAE workflow with comprehensive UPLC-Q-TOF-MS/MS profiling, identifying 32 constituents, and targeted HPLC quantification of six major phenolic glycoside compounds. Different from many earlier studies adopting only one or two simple bioassays, three functionally interconnected in vitro cell models were deployed in this work, covering ethanol-induced hepatocyte injury, intracellular antioxidant biomarker detection, and LPS-provoked macrophage inflammatory response to systematically characterize extract bioactivity. Moreover, the adopted 65% aqueous ethanol system avoids toxic methanol and reduces solvent consumption relative to pharmacopoeia-documented sonication and reported microwave-assisted extraction strategies. It should be noted that the green-related performance described herein is only approximate; a formal life-cycle assessment is required for further industrial translation.

Nevertheless, several limitations remain. No dedicated positive reference compound was included in the anti-inflammatory cell assay; further work is needed to validate bioactivity with appropriate positive controls. Future investigations should focus on isolation and bio-testing of individual characteristic constituents from GE-UAE, in vivo animal verification of hepatoprotective and anti-inflammatory effects, and evaluation of extract scalability, stability, and formulation feasibility for nutraceutical development.

Author Contributions: J.L.: Writing—original draft, validation, methodology, and conceptualization. H.L.: Resources, writing—review and editing, project administration, and methodology. H.Z.: Methodology and investigation. D.L.: Methodology and investigation. H.J.: Supervision, project administration, and funding acquisition. All authors have read and agreed to the published version of the manuscript.

Funding: This research was funded by the Local Financial Funds of the National Agricultural Science and Technology Center, Chengdu (No. NASC2024KR22), the Local Financial Funds of National Agricultural Science and Technology Center, Chengdu (No. NASC2024NR0802), the Agricultural Science and Technology Innovation Program of the Chinese Academy of Agricultural Sciences (No. ASTIP2026-34-IUA-09), and the Major Tasks at the Institute of Urban Agriculture, Chinese Academy of Agricultural Sciences (SZ202403).

Data Availability Statement: The original contributions presented in this study are included in the article. Further inquiries can be directed to the corresponding author.

Acknowledgments: The authors thank all members of the research group for their support during sample preparation and data processing.

Conflicts of Interest: The authors declare that they have no known competing financial interests or personal relationships that could have appeared to influence the work reported in this paper.

References

1. Yang, Y.; Hai, Y.; Yang, Y.; Wen, R.; Wang, L.; Qian, Y.; Zhang, J.; Li, Y.; Shi, Z.; Zhang, H. Extraction, purification, structural characteristics, biological activities, and applications of polysaccharides from *Gastrodia elata*: A review. *Molecules* **2025**, *30*, 262. [CrossRef]
2. Li, C.; Li, J.; Wang, Y.-Z. A review of *Gastrodia elata* Bl.: Extraction, analysis and application of functional food. *Crit. Rev. Anal. Chem.* **2024**, *56*, 179–208. [CrossRef]
3. Su, Z.; Yang, Y.; Chen, S.; Tang, Z.; Xu, H. The processing methods, phytochemistry and pharmacology of *Gastrodia elata* Bl.: A comprehensive review. *J. Ethnopharmacol.* **2023**, *314*, 116467. [CrossRef]
4. Su, Z.; Yang, Y.; Xu, H.; Tang, Z.; Sun, M.; Zhu, Y.; Xue, T.; He, Y.; Wang, H.; Yang, H.; et al. Study on the chemical composition and in vitro enzyme inhibition of different processed products of *Gastrodia elata*. *J. Food Compos. Anal.* **2024**, *130*, 106148. [CrossRef]
5. Yu, H.; Zhang, J.; Chen, B.Q.; Huang, H.; Li, Z.H.; Huang, S.W.; Li, X.X.; Liu, X.M.; Lyu, G.H. Research progress on classification of chemical constituents from *Gastrodia elata* and their pharmacological effects. *Chin. Tradit. Herb. Drugs* **2022**, *53*, 5553–5564. [CrossRef]
6. Li, X.; Wu, Z.; Yang, Y.; Chen, G.; Zhang, Y. The differences in total polyphenols and total flavonoids content in *Gastrodia elata* Bl. f. glauca S. Chow extracts using different solvent and their antioxidant capacities. *Food Ferment. Ind.* **2022**, *48*, 157–164. [CrossRef]
7. Zheng, X.; Gong, T.; Yu, W.; Xu, S.; Tang, C.; Zhong, Y.; Zhu, Z. Study on cellular mechanism of improving inflammatory effect of gastrodin. *Tohoku J. Exp. Med.* **2025**, *265*, 249–259. [CrossRef]
8. El Menyiy, N.; Elouafy, Y.; Moubachir, R.; Abdnim, R.; Benali, T.; Taha, D.; Khalid, A.; Abdalla, A.N.; Hamza, S.M.A.; Elhadi Ibrahim, S.; et al. Chemistry, biological activities, and pharmacological properties of gastrodin: Mechanism insights. *Chem. Biodivers.* **2024**, *21*, e202400402. [CrossRef]
9. Ahmad, O.; Wang, B.; Ma, K.; Deng, Y.; Li, M.; Yang, L.; Yang, Y.; Zhao, J.; Cheng, L.; Zhou, Q.; et al. Lipid modulating anti-oxidant stress activity of gastrodin on nonalcoholic fatty liver disease larval zebrafish model. *Int. J. Mol. Sci.* **2019**, *20*, 1984. [CrossRef]
10. Xiao, G.; Tang, R.; Yang, N.; Chen, Y. Review on pharmacological effects of gastrodin. *Arch. Pharmacal Res.* **2023**, *46*, 744–770. [CrossRef]
11. Kumar, M.; Dahuja, A.; Tiwari, S.; Punia, S.; Tak, Y.; Amarowicz, R.; Bhoite, A.G.; Singh, S.; Joshi, S.; Panesar, P.S.; et al. Recent trends in extraction of plant bioactives using green technologies: A review. *Food Chem.* **2021**, *353*, 129431. [CrossRef]
12. Wani, K.M.; Uppaluri, R.V.S. Efficacy of ultrasound-assisted extraction of bioactive constituents from *Psidium guajava* leaves. *Appl. Food Res.* **2022**, *2*, 100096. [CrossRef]
13. Addo, P.W.; Sagili, S.U.K.R.; Bilodeau, S.E.; Gladu-Gallant, F.-A.; MacKenzie, D.A.; Bates, J.; McRae, G.; MacPherson, S.; Paris, M.; Raghavan, V.; et al. Microwave- and ultrasound-assisted extraction of cannabinoids and terpenes from cannabis using response surface methodology. *Molecules* **2022**, *27*, 8803. [CrossRef]
14. Shao, J.; Xiao, X.; Li, Y.; Chen, B.; Xing, L.; Zhu, Z.; Qi, C. Ultrasound-assisted enzymatic extraction of dark tea total polyphenols. *Front. Nutr.* **2025**, *12*, 1548103. [CrossRef]
15. Wu, D.-T.; Deng, W.; Li, J.; Geng, J.-L.; Hu, Y.-C.; Zou, L.; Liu, Y.; Liu, H.-Y.; Gan, R.-Y. Ultrasound-assisted deep eutectic solvent extraction of phenolic compounds from thinned young kiwifruits and their beneficial effects. *Antioxidants* **2023**, *12*, 1475. [CrossRef]
16. Li, X.; Li, X.; Deng, Y.; Chen, L.; Zheng, Z.; Ming, Y. Protective effect of corilagin on alcoholic liver injury. *Nat. Prod. Commun.* **2024**, *19*, 9. [CrossRef]
17. Che, H.; Zhang, R.; Wang, X.; Yu, H.; Shi, X.; Yi, J.; Li, J.; Qi, Q.; Dong, R.; Li, Q. Ultrasound-assisted extraction of polyphenols from Phyllanthi Fructus: Comprehensive insights from extraction optimization and antioxidant activity. *Ultrason. Sonochem.* **2024**, *111*, 107083. [CrossRef]
18. Li, G.; Bao, C.; Zhang, H.; Bai, L. Ultrasound-assisted extraction of polyphenols from Lonicera japonica leaves and their α-glucosidase inhibition. *Front. Nutr.* **2025**, *12*, 1542217. [CrossRef]
19. Zhang, S.; Xie, H.; Huang, J.; Chen, Q.; Li, X.; Chen, X.; Liang, J.; Wang, L. Ultrasound-assisted extraction of polyphenols from pine needles (*Pinus elliottii*): Comprehensive insights from RSM optimization, antioxidant activity, UHPLC-Q-Exactive Orbitrap MS/MS analysis and kinetic model. *Ultrason. Sonochem.* **2024**, *102*, 106742. [CrossRef]
20. Huaman-Castilla, N.L.; Martínez-Cifuentes, M.; Camilo, C.; Pedreschi, F.; Mariotti-Celis, M.; Pérez-Correa, J.R. The impact of temperature and ethanol concentration on the global recovery of specific polyphenols in an integrated HPLE/RP process on Carménère pomace extracts. *Molecules* **2019**, *24*, 3145. [CrossRef]

21. Sun, Y.; Lu, J.; Li, J.; Li, P.; Zhao, M.; Xia, G. Optimization of ultrasonic-assisted extraction of polyphenol from Areca nut (*Areca catechu* L.) seeds using response surface methodology and its effects on osteogenic activity. *Ultrason. Sonochem.* **2023**, *98*, 106511. [CrossRef]
22. Metrouh-Amir, H.; Duarte, C.M.M.; Maiza, F. Solvent effect on total phenolic contents, antioxidant, and antibacterial activities of Matricaria pubescens. *Ind. Crops Prod.* **2015**, *67*, 249–256. [CrossRef]
23. Leng, X.; Miao, W.; Li, J.; Liu, Y.; Zhao, W.; Mu, Q.; Li, Q. Physicochemical characteristics and biological activities of grape polysaccharides collected from different cultivars. *Food Res. Int.* **2023**, *163*, 112161. [CrossRef]
24. Li, J.; Chen, Z.; Shi, H.; Yu, J.; Huang, G.; Huang, H. Ultrasound-assisted extraction and properties of polysaccharide from *Ginkgo biloba* leaves. *Ultrason. Sonochem.* **2023**, *93*, 106295. [CrossRef]
25. Wen, Y.; Zeng, X.; Mai, X. Optimization of ultrasonic-assisted extraction and biological activities of total polyphenols from *Toona sinensis* using response surface methodology. *Biomass Convers. Biorefin.* **2024**, *14*, 14225–14238. [CrossRef]
26. Yang, Y.; Han, K.; Liu, Z.; Xie, S.; Xu, J.; He, Y.; Zhao, P.; Yang, X. Ultrasonic-assisted biphasic aqueous extraction of polyphenols from *Vaccinium dunalianum* leaves: Optimization, antioxidant, and tyrosinase inhibition activities. *Chem. Biodivers.* **2024**, *21*, e202400955. [CrossRef]
27. Hu, T.; Wang, F.; Zhao, Z.; Hu, K.; Zhou, C. Optimization, purification and antioxidant potential of polyphenol ultrasonic-assisted extraction from pecan 'Shaoxing' green husk. *Food Prod. Process. Nutr.* **2025**, *7*, 20. [CrossRef]
28. Wu, D.-T.; Feng, K.-L.; Huang, L.; Gan, R.-Y.; Hu, Y.-C.; Zou, L. Deep eutectic solvent-assisted extraction, partially structural characterization, and bioactivities of acidic polysaccharides from Lotus leaves. *Foods* **2021**, *10*, 2330. [CrossRef]
29. Wu, D.-T.; Geng, J.-L.; Li, J.; Deng, W.; Zhang, Y.; Hu, Y.-C.; Zou, L.; Xia, Y.; Zhuang, Q.-G.; Liu, H.-Y.; et al. Efficient extraction of pectic polysaccharides from thinned unripe kiwifruits by deep eutectic solvent-based methods: Chemical structures and bioactivities. *Food Chem. X* **2024**, *21*, 101083. [CrossRef]
30. Hu, M.; Yan, H.; Fu, Y.; Jiang, Y.; Yao, W.; Yu, S.; Zhang, L.; Wu, Q.; Ding, A.; Shan, M. Optimal Extraction Study of Gastrodin-Type Components from *Gastrodia elata* Tubers by Response Surface Design with Integrated Phytochemical and Bioactivity Evaluation. *Molecules* **2019**, *24*, 547. [CrossRef]
31. Zhang, J.; Zhang, D.; Qin, J. *Optimization of Gastrodin and Gastrodigenin Extraction Technology and Effect of Different Harvest Festivals on Their Contents*; SPIE: Bellingham, WA, USA, 2013; Volume 8762.
32. Wang, Y.; Zhong, L.; Fang, H.; Liu, Z.; Wang, P.; Li, L.; Chen, L.; Ding, G. Bioactive metabolites from the dusty seeds of *Gastrodia elata* Bl., based on metabolomics and UPLC-Q-TOF-MS combined with molecular network strategy. *Plants* **2025**, *14*, 916. [CrossRef]
33. Qian, C.-Q.; Yang, Y.-W.; Meng, Y.; Dai, S.-H.; Tao, J.; Dong, H. Chemical composition analysis and quality identification of gastrodia tuber in tibet based on HPLC-MS. *Prog. Mod. Biomed.* **2014**, *14*, 611–616+649. (In Chinese). Available online: http://biomed.cnjournals.com/ch/reader/view_abstract.aspx?file_no=201404003&flag=1 (accessed on 1 September 2026).
34. Li, B.; Bai, J.; He, W.; Wang, X.; Zhang, W.; Yang, Q. Analysis of chemical components in the stem and tuber of *Gastrodia elata* f. glauca using UPLC-Q-TOF-MS/MS. *Mod. Chin. Med.* **2024**, *44*, 99–105. [CrossRef]
35. Zhang, S.; Du, W.; Dong, H. Study on the transition components of Tianma Gouteng Yin in vitro and in rat blood based on UPLC/Q-TOF MS technology. *J. Li-Shizhen Tradit. Chin.* **2021**, *32*, 1115–1119. (In Chinese). Available online: https://www.sinomed.ac.cn/article.do?ui=2021480416 (accessed on 1 September 2026).
36. Dai, H.; Hou, X.; Jiang, W.; Zhou, L.; Mou, H.; Hou, C.; Zhang, J. Exploring the mechanism of sedative and hypnotic effects of bijie red gastrodiae rhizoma based on UPLC-Q-TOF/MS technology and network pharmacology. *Tradit. Chin. Drug Res. Clin. Pharmacol.* **2026**, *37*, 82–94. (In Chinese) [CrossRef]
37. Wen, L.; Jiang, Y.; Wang, W.; Zhu, R.; Liu, J.; He, Y.; Zheng, F.; Wu, Y. Chemical composition, biological activities and product development of *Gastrodia elata*: A review. *Food Sci. Hum. Wellness* **2025**, *14*, 9250226. [CrossRef]
38. Georgé, S.; Brat, P.; Alter, P.; Amiot, M.J. Rapid determination of polyphenols and vitamin C in plant-derived products. *J. Agric. Food Chem.* **2005**, *53*, 1370–1373. [CrossRef]
39. Chen, X.; Yi, P.; Lv, H.; Zhang, M.; Yang, J.; Zhang, Z.; Zhao, Z.; Mu, Y.; Han, L.; Huang, X. Phenolics and phenolic glycosides from wrightia pubescens and their hepatoprotective activities. *J. Nat. Prod.* **2025**, *88*, 631–643. [CrossRef]
40. Zhou, Y.; Jin, H.; Wu, Y.; Chen, L.; Bao, X.; Lu, C. Gallic acid protects against ethanol-induced hepatocyte necroptosis via an NRF2-dependent mechanism. *Toxicol. Vitr.* **2019**, *57*, 226–232. [CrossRef]
41. Zhang, Y.; Wang, C.; Yu, B.; Jiang, J.-D.; Kong, W.-J. Gastrodin protects against ethanol-induced liver injury and apoptosis in HepG2 cells and animal models of alcoholic liver disease. *Biol. Pharm. Bull.* **2018**, *41*, 670–679. [CrossRef]
42. Lu, J.-Y.; Zuo, H.-T.; Feng, R.; Chen, Y.-L.; Ye, M.-L.; Xu, H.; Hu, J.-C.; Song, J.-Y.; Zhao, Y.; Wang, J.-Y.; et al. Parishin A reduces hepatic encephalopathy via gut microbiota increasing the activity of intestinal EAAT3 to reduce blood ammonia. *Pharmacol. Res.* **2025**, *222*, 108030. [CrossRef]
43. Tian, Z.K.; Zhang, Y.J.; Feng, Z.J.; Jiang, H.; Cheng, C.; Sun, J.M.; Liu, C.M. Nephroprotective effect of gastrodin against lead-induced oxidative stress and inflammation in mice by the GSH, Trx, Nrf2 antioxidant system, and the HMGB1 pathway. *Toxicol. Res.* **2021**, *10*, 249–263. [CrossRef]

44. Sergent, O.; Griffon, B.; Cillard, P.; Cillard, J. Alcool et stress oxydatif Alcohol and oxidative stress. *Pathol. Biol.* **2001**, *49*, 689–695. [CrossRef]
45. Dey, A.; Cederbaum, A.I. Alcohol and oxidative liver injury. *Hepatology* **2006**, *43*, S63–S74. [CrossRef]
46. Berköz, M.; Aslan, A.; Yunusoglu, O.; Krosniak, M.; Francik, R. Hepatoprotective potentials of *Usnea longissima* Ach. and *Xanthoparmelia somloensis* (Gyelnik) Hale extracts in ethanol-induced liver injury. *Drug Chem. Toxicol.* **2025**, *48*, 136–149. [CrossRef]
47. Liang, H.-W.; Yang, T.-Y.; Teng, C.-S.; Lee, Y.-J.; Yu, M.-H.; Lee, H.-J.; Hsu, L.-S.; Wang, C.-J. Mulberry leaves extract ameliorates alcohol-induced liver damages through reduction of acetaldehyde toxicity and inhibition of apoptosis caused by oxidative stress signals. *Int. J. Med. Sci.* **2021**, *18*, 53–64. [CrossRef]
48. Qin, F.; Yao, L.; Lu, C.; Li, C.; Zhou, Y.; Su, C.; Chen, B.; Shen, Y. Phenolic composition, antioxidant and antibacterial properties, and in vitro anti-HepG2 cell activities of wild apricot (*Armeniaca sibirica* L. Lam) kernel skins. *Food Chem. Toxicol.* **2019**, *129*, 354–364. [CrossRef]
49. Wu, S.; Wu, X.; Huang, F.; Zheng, J. Research progress on the efficacy and processing stability of the major active ingredients in *Gastrodia elata* Bl. *Food Sci.* **2025**, *46*, 363–371. (In Chinese) [CrossRef]
50. Yao, Y.-Y.; Li, R.; Guo, Y.-J.; Zhao, Y.; Guo, J.-Z.; Ai, Q.-L.; Zhong, L.-M.; Lu, D. Gastrodin attenuates lipopolysaccharide-induced inflammatory response and migration *via* the notch-1 signaling pathway in activated microglia. *NeuroMolecular Med.* **2022**, *24*, 139–154. [CrossRef]
51. Xue, X.; Li, F.; Xu, M.; Chen, B.; Zhao, Y.; Wang, M.; Li, L. Gastrodin ameliorates atherosclerosis by inhibiting foam cells formation and inflammation through down-regulating NF-κB pathway. *Nutr. Metab.* **2023**, *20*, 9. [CrossRef]

Disclaimer/Publisher's Note: The statements, opinions and data contained in all publications are solely those of the individual author(s) and contributor(s) and not of MDPI and/or the editor(s). MDPI and/or the editor(s) disclaim responsibility for any injury to people or property resulting from any ideas, methods, instructions or products referred to in the content.